Order-Disorder Transitions in the Melt Morphology of Laser-Irradiated Silicon

J. S. Preston, H. M. van Driel, and J. E. Sipe
Department of Physics and Erindale College, University of Toronto, Toronto, Ontario, Canada M5S 1A7
(Received 19 May 1986)

The melting of thin silicon films with continuous laser radiation is characterized by the formation of several distinct and reproducible microscopic patterns of solid and molten regions with various degrees of long-range order. The pattern formation reflects the competition between the coherent energy deposition from the laser beam and the incoherent heat loss via diffusion. A phase, or stability, diagram of the structures has been constructed and order-disorder nonequilibrium "phase" transitions between these melt morphologies have been demonstrated by changes of the laser intensity and/or spot size.

PACS numbers: 79.20.Ds, 05.70.Ln, 64.70.Dv, 81.40.Gh

Nature has provided many examples of spatial and temporal patterns which develop in physical, chemical, biological, and even sociological systems under nonequilibrium conditions.[1] In this Letter, we show how instabilities in the optical response of Si can lead to the formation of several distinct microscopic patterns of coexisting solid and molten regions during cw (continuous wave) laser melting. These patterns are distinguishable on the basis of symmetry properties, order versus disorder, and the fraction of the surface that is molten. The structures are also significant in that they not only result from a fundamental process (optical heating), but also because their form and symmetry are independent of the explicit boundary conditions. Anderson[2] has noted that other nonequilibrium systems seldom, if ever, exhibit such properties.

Explanations of the solid and/or molten phases previously observed[3-5] have concentrated on an instability which arises because of the abrupt increase in the bulk reflectivity of Si upon melting. This results in a range of intensities for which a solid surface would be overheated while a molten surface would be undercooled.[5-7] (It has been noted[8] that this argument, which is based on bulk properties, must be modified slightly if optically thin molten regions develop, since the reflectivity then varies continuously with the melt because of skin-depth effects.) This instability would of itself lead to limit-cycle behavior in which the surface would alternatively melt and resolidify. However, the coherence of laser light leads to an additional *transverse* instability due to the interference of the incident and a surface scattered beam. This other instability is responsible for breaking the translational symmetry of the surface. The final steady-state pattern depends upon the competition between the coherent energy deposition and the removal and redistribution of energy due to thermal conduction. This differs from the case of pulsed-laser–induced periodic structures where heat flow is negligible and the pattern formation is determined solely by the interference mechanisms.[9-11]

Our experiments were conducted with the use of a linearly polarized 20-W cw CO_2 laser operating in TEM_{00} mode at $\lambda = 10.6\ \mu$m. The samples used were 2-μm-thick Si films on sapphire substrates. The location and size of the irradiated spot could be manipulated with the use of a 10-cm focal length ZnSe lens. The sample's own blackbody emission was used to view the melt patterns through the back of the sapphire substrates by use of a 20× microscope objective. Simple estimates indicate that thermal conduction into the sapphire is the dominant heat-loss mechanism but the two most salient experimental parameters which determine the microstructures are the incident intensity and the lateral heat flow. The latter can be adjusted by changes of the laser spot size and hence the lateral temperature gradient. Patterns formed for two different intensities and spot sizes are shown in Fig. 1. Figure 1(a) exhibits two different, ordered gratinglike structures, one of which, with a spacing of λ covers most of the area, while another grating structure with spacing 2λ occurs at the center of the spot where the local intensity is higher. Figure 1(b) depicts a more disordered pattern consisting of irregular lamellae which form for lower laser intensities and larger spot sizes.

In Fig. 2 we summarize in a stability or "phase" diagram the different nonequilibrium states associated with a given incident intensity and spot size. Region I is the solid phase of Si while region II consists of an irregular distribution of isolated molten regions approximately 34 μm in diameter. Since this structure is observed only over a narrow range of intensities, and hence only over small geometric areas, region II may not be a phase of the infinite system but rather an artifact of the spot size. In regions III and IV, periodic structures with wave vector κ oriented parallel to the incident polarization are formed. Within experimental error, the spacing of the gratings ($2\pi\kappa^{-1}$) is equal to λ in region III and 2λ in region IV, as is shown in Fig. 1(a). Observations of the transition from region III to region IV have revealed that alternate solid strips melt during the period doubling. Gratings with period 3λ, 4λ, etc., occur in region V. In region VI, the patterns of liquid and solid [see Fig. 1(b)] have an average spacing of several micrometers which is governed by thermal and mechanical parameters such as surface ten-

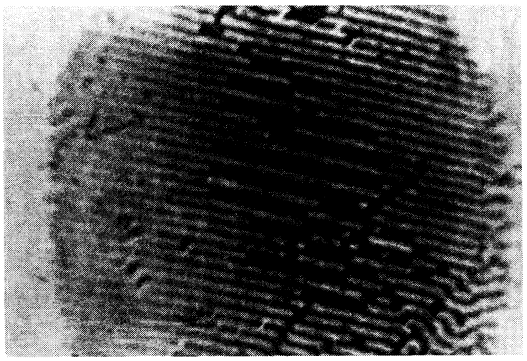

(a)

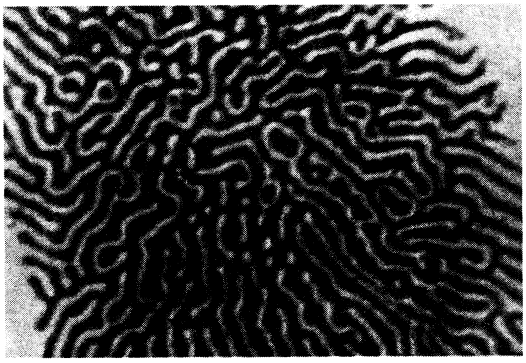

(b)

FIG. 1. Photographs depicting different molten morphological structures formed under conditions of (a) 3.2 kW/cm^2, 500-μm-diam spot; (b) 1.7 kW/cm^2, 700-μm-diam spot. Spatial variations are on a scale of $\lambda = 10.6$ μm; dark regions are molten. Note the period doubling in the center of (a).

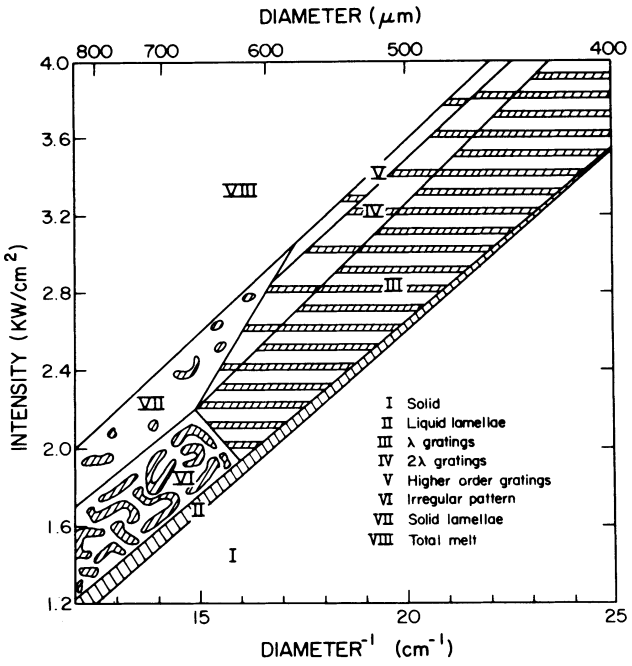

FIG. 2. Nonequilibrium phase diagram for silicon under laser irradiation at 10.6 μm.

sion. Also within region VI, the morphology of the structure undergoes a rather subtle transition from isolated liquid regions to isolated solid regions as the intensity increases. Finally, in region VII the solid regions become separated by more than λ. The isolated lamellae, i.e., their temperature fields, then appear to move independently, interacting only if the separation becomes comparable to λ.

The phase diagram indicates that the gratinglike structures are associated with relatively small spot sizes and hence larger heat loss than the disordered ("amorphous") structures. Because of the higher intensities required to initiate melting in smaller spots for which the transverse temperature gradients are larger, coherent power deposition is more effective in ordering the surface. Figure 2 also indicates that the fraction of liquid increases with laser intensity as expected. However, from Fig. 3(a), which shows the fraction of liquid (f_m) as a function of laser intensity for a spot size associated with grating structures, there are discrete jumps in f_m which occur solely as a result of the change in grating periodicity. Changes in the width of the solid regions were found to be negligible, resulting in the striking plateaus. We can thus identify f_m as an order parameter whose change marks a transition between highly stable morphological phases. In the corresponding plot for the "amorphous" structures, Fig. 3(b), the fraction of liquid increases smoothly although some remnant of the plateaus remain.

Any fundamental understanding of this system's evolution requires a description of the coupling of the incident fields to the surface structures. In the geometric-optics limit, relatively little energy is deposited in the melt since the reflectivity is so high. If one assumes that the energy is deposited preferentially in the solid, the surface morphology must then consist of rather unconventional boundaries between supercooled molten regions and superheated solid regions.[5] Jackson and Kurtze[7] have argued that such a boundary between two unstable phases can in fact be stabilized by surface tension. However, for melt structures with size on the order of λ, geometrical optics is not a good approximation, and previous arguments[3-7] based on its application are not valid.

To address correctly the issue of energy deposition, a physical-optics theory is required. In particular, we require an electrodynamic theory which takes into account the large differences in the solid and melt optical properties, and allows for interference between the incident beam and scattered fields. To do this we approximate the response of the surface to the incident radiation by a uniform polarization within the solid regions and current

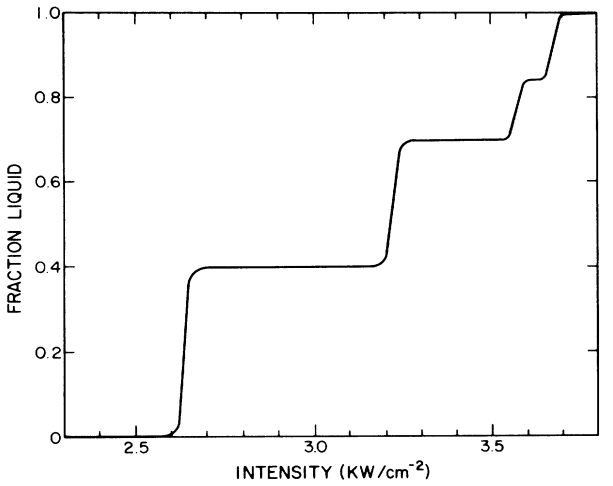

(a)

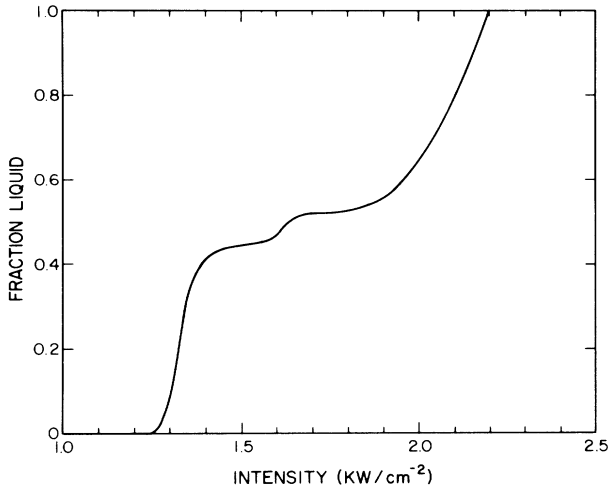

(b)

FIG. 3. The fraction of liquid vs the laser intensity for a spot size of (a) 500 μm and (b) 800 μm.

densities at the vacuum-melt and melt-substrate interfaces. The condition that the electric and magnetic fields vanish in the interior of the metallic molten regions is used to calculate the values of these parameters. Once the polarization and current densities are known it is straightforward to calculate the fields produced and the energy dissipated. While details of the above approach will be discussed elsewhere, some results can be presented here which illustrate the existence of the various grating structures. For simplicity we consider a free-standing film (no substrate) consisting of a solid-liquid grating of wave vector κ with the sample half molten. We consider only the leading term in a Fourier expansion of the liquid-solid correlation function of the surface. In the case of linearly polarized light of field strength E_0 normally incident on the grating with $\phi=\angle(\mathbf{E}_0,\boldsymbol{\kappa})=0°$ the expressions for the magnitude of the top and bottom interface current densities, K^t, K^b, and the field E in the solid are given by

$$-i\omega K^t=\frac{c}{4\pi}\left[\frac{3\tilde{\omega}+(\tilde{\omega}^2-\kappa^2)^{1/2}}{\tilde{\omega}+(\tilde{\omega}^2-\kappa^2)^{1/2}}\right]E_0,$$

$$K^b=\frac{c}{4\pi}\left[\frac{\tilde{\omega}-(\tilde{\omega}^2-\kappa^2)^{1/2}}{\tilde{\omega}+(\tilde{\omega}^2-\kappa^2)^{1/2}}\right]E_0,$$

$$E=\left[\frac{2(\tilde{\omega}^2-\kappa^2)^{1/2}}{(\tilde{\omega}+(\tilde{\omega}^2-\kappa^2)^{1/2}}\right]E_0,$$

where $\tilde{\omega}=\omega/c$ and ω is the frequency of the incident light. Different expressions exist for the fields oriented parallel to the grating or $\phi=90°$. These expressions can be used to calculate the correction required to the geometric-optics limit ($\kappa=0$) for the energy deposited in the molten and solid regions. This is shown in Fig. 4 for the two field orientations. For $\phi=0°$ and $\kappa\neq0$, the power deposited in the melt is dramatically enhanced, while the power deposited in the solid regions is suppressed leading to the power being deposited primarily in the molten regions. As κ approaches $\tilde{\omega}$ (grating spacing approaches in-

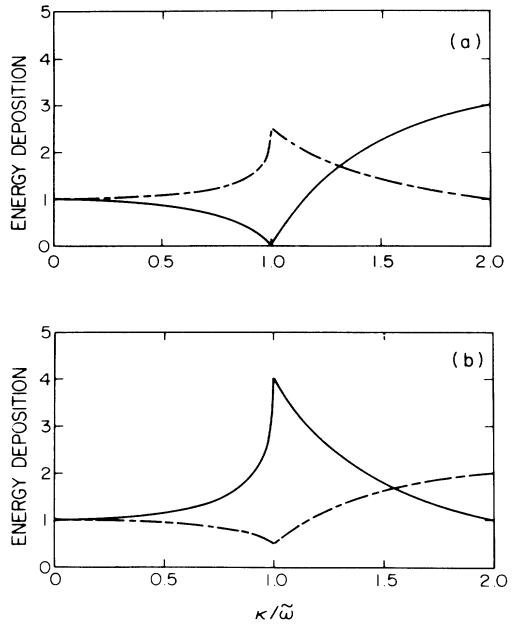

FIG. 4. The ratio of the actual power deposition to that of the geometric-optics limit for a grating structure of wave vector κ oriented parallel ($\phi=0°$) and perpendicular ($\phi=90°$) to the polarization. The dashed and solid lines refer to the molten and solid regions, respectively.

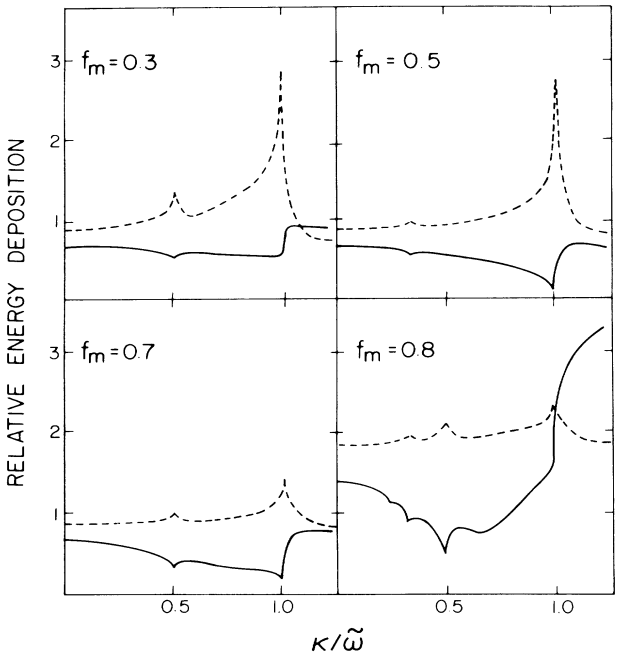

FIG. 5. Relative power deposition in the molten (dashed curve) vs solid (solid curve) regions of a grating on a sapphire substrate as a function of normalized wave number with different fractions (f_m) of the surface molten.

cident wavelength), the relative power deposition in the molten and solid regions are a maximum and minimum, respectively. Although the fields are confined to the surface of the molten regions, constructive interference between the scattered and incident fields greatly enhances the energy deposited. In the solid regions the fields interfere destructively leading to a phenomena which we have labeled "interference shielding." Through this mechanism the melt is maintained at a higher temperature than the solid, leading to a conventional interface.

While inclusion of the substrate does not lead to any qualitative changes, retention of the higher Fourier components of the liquid-solid correlation function leads to new peaks in the energy deposition at $\tilde{\kappa}=\kappa/\tilde{\omega}=1/n$, where n is an integer. These peaks occur whenever one of the Fourier component frequencies matches the wave number of the incident (scattered) light and gratings at 2λ, 3λ, etc., can result. (Note that the existence of higher-order gratings leading to full melting is not associated with period doubling and chaos phenomena as the existence of a 3λ grating alone would argue against.) In Fig. 5, the corrections to the geometric-optics limit are shown for gratings of variable κ with different f_m (the equations above have been modified to general f_m). The amount of shielding of the solid regions is a sensitive function of f_m. For a grating with a spacing of λ, the shielding is most efficient when the surface is 50% molten. As f_m increases the shielding becomes less efficient until $f_m \simeq 0.8$ when it is clear that the doubled grating is much more efficient at shielding the solid regions.

We would like to acknowledge the generosity of D. Biegelsen and D. Guidotti for providing the silicon-on-sapphire samples used in this work. This work is supported by the Natural Sciences and Engineering Research Council of Canada, including a postgraduate scholarship to one of us (J.P.).

[1]*Pattern Formation by Dynamic Systems and Pattern Recognition*, edited by H. Haken (Springer-Verlag, New York, 1979); G. Nicholis and I. Prigogine, in *Self-Organization in Non-Equilibrium Systems* (Wiley, New York, 1977); D. Walgraef, G. Dewel, and P. Borckmans, Adv. Chem. Phys. **49**, 311 (1982).

[2]P. W. Anderson, in *Order and Fluctuations in Equilibrium and Non-Equilibrium Statistical Mechanics*, edited by G. Nicholis, G. Dewel, and J. W. Turner (Wiley-Interscience, New York, 1981).

[3]M. A. Bosch and R. A. Lemons, Phys. Rev. Lett. **47**, 1151 (1981).

[4]R. J. Nemanich, D. K. Biegelsen, and W. G. Hawkins, in *Laser and Electron-Beam Interactions with Solids*, edited by B. R. Appleton and G. K. Celler (North-Holland, New York, 1982), p. 211.

[5]W. G. Hawkins and D. K. Biegelsen, Appl. Phys. Lett. **42**, 358 (1983).

[6]M. Combescot, J. Bok, and C. Benoit à la Guillaume, Phys. Rev. B **29**, 6393 (1985).

[7]K. A. Jackson and Douglas A. Kurtze, J. Cryst. Growth **71**, 385 (1985).

[8]J. E. Sipe, J. F. Young, and H. M. van Driel, in *Laser-Controlled Chemical Processing of Surface*, edited by A. W. Johnson, D. J. Ehrlich, and H. R. Scholssberg (North-Holland, New York, 1984), p. 415.

[9]J. F. Young, J. E. Sipe, M. I. Gallant, J. S. Preston, and H. M. van Driel, in *Laser and Electron-Beam Interactions with Solids*, edited by B. R. Appleton and G. K. Celler (North-Holland, New York, 1982), p. 233.

[10]J. E. Sipe, J. F. Young, J. S. Preston, and H. M. van Driel, Phys. Rev. B **27**, 1411 (1983).

[11]P. M. Fauchet, Z. Guosheng, and A. E. Siegman, in *Laser-Solid Interactions and Transient Thermal Processing of Materials*, edited by J. Narayan, W. L. Brown, and R. A. Lemons (North-Holland, New York, 1983), p. 205.

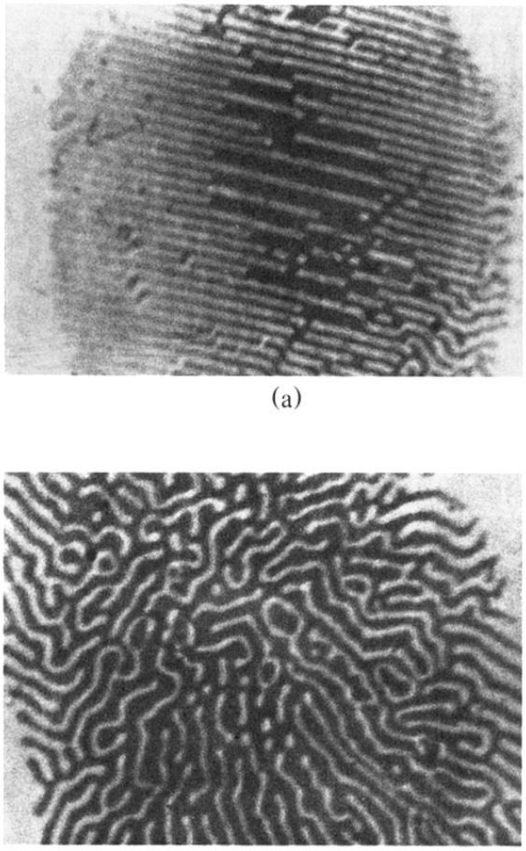

(a)

(b)

FIG. 1. Photographs depicting different molten morphological structures formed under conditions of (a) 3.2 kW/cm^2, 500-μm-diam spot; (b) 1.7 kW/cm^2, 700-μm-diam spot. Spatial variations are on a scale of $\lambda = 10.6$ μm; dark regions are molten. Note the period doubling in the center of (a).